AGU PUBLICATIONS

JGR

Journal of Geophysical Research: Space Physics

RESEARCH ARTICLE

10.1002/2014JA020805

Key Points:
- A comprehensive survey of 300 events of 3 day planetary-scale waves in the MLT
- Quantify importance and frequency of 3 day wave impact on equatorial ionosphere
- No season/solar cycle dependence of 3 day wave propagation above mesopause

Correspondence to:
G. Liu,
guiping@ssl.berkeley.edu

Citation:
Liu, G., S. L. England, T. J. Immel, H. U. Frey, A. J. Mannucci, and N. J. Mitchell (2015), A comprehensive survey of atmospheric quasi 3 day planetary-scale waves and their impacts on the day-to-day variations of the equatorial ionosphere, *J. Geophys. Res. Space Physics*, *120*, 2979–2992, doi:10.1002/2014JA020805.

Received 6 NOV 2014
Accepted 2 MAR 2015
Accepted article online 7 MAR 2015
Published online 1 APR 2015

A comprehensive survey of atmospheric quasi 3 day planetary-scale waves and their impacts on the day-to-day variations of the equatorial ionosphere

Guiping Liu[1], Scott L. England[1], Thomas J. Immel[1], Harald U. Frey[1], Anthony J. Mannucci[2], and Nicholas J. Mitchell[3]

[1]Space Sciences Laboratory, University of California, Berkeley, California, USA, [2]Jet Propulsion Laboratory, California Institute of Technology, Pasadena, California, USA, [3]Centre for Space, Atmospheric and Oceanic Science, Department of Electronic and Electrical Engineering, University of Bath, Bath, UK

Abstract This study reports a comprehensive survey of quasi 3 day (2.5–4.5 day period) planetary-scale waves in the low-latitude mesosphere and lower thermosphere using the temperature observations from Thermosphere Ionosphere and Mesosphere Electric Dynamics/Sounding of the Atmosphere using Broadband Emission Radiometry throughout 2002–2012. Occurrences and properties of the waves, including the eastward propagating zonal wave numbers of 1–3 (*E*1–*E*3) and vertical wavelengths, are determined for each case. The impacts of these waves on the equatorial ionosphere are investigated by searching for the corresponding variations with the same periods and wave numbers in total electron content (TEC) from the concurrent observations of the ground-based GPS network. For a threshold amplitude of 4 K in temperature, a total of 300 waves are identified, of which there are 186 *E*1, 63 *E*2, and 51 *E*3 events. The mean amplitudes and vertical wavelengths of these waves are calculated to be about 7.9 K and 34 km for the *E*1, 5.7 K and 29 km for the *E*2, and 5.1 K and 27 km for the *E*3, having the standard deviations of 1.5 K and 6.5 km, 0.6 K and 5.6 km, and 0.5 K and 6.7 km. Occurrences of the *E*1 cases are not observed to depend on season, but the large-amplitude (>8 K) cases occur more often during solstices than at equinoxes. Similarly, the *E*2 and *E*3 cases are observed to occur most often in January–February and May–August. Among these waves, 199 cases (66%) are found to have the corresponding variations in the equatorial ionosphere with amplitudes ≥4.2% relative to the mean TEC values (corresponding to 90th percentile). Most of these waves have long vertical wavelengths and large amplitudes (~3 times more than short vertical wavelength and small-amplitude waves). Because no seasonal or solar cycle dependence on the frequency at which these waves have corresponding variations in the ionosphere at this TEC perturbation threshold is observed, we conclude that there is no seasonal and solar cycle dependence on the propagation of such waves from the mesopause region to higher altitudes. We also identify that only 28 cases (19%) of the *E*1 TEC variations do not correspond to any *E*1 waves, which is consistent with the hypothesis that *E*1 waves are the primary cause of *E*1 TEC variations. Conditions that are favorable for 3 day waves to create ionospheric variations are present approximately two thirds of the time. This study quantifies the importance and frequency of atmospheric quasi 3 day planetary-scale waves on the day-to-day variations of the equatorial ionosphere using a statistical rather than case study approach.

1. Introduction

Planetary-scale waves are believed to play an important role in coupling the atmosphere to the ionosphere. Even at geomagnetic and solar quiet conditions, the equatorial ionosphere has been found to exhibit a large day-to-day variability [e.g., *Laštovička*, 2006]. Much of this variability has been attributed to the forcing by atmospheric planetary-scale waves with periods of 2–16 days [e.g., *Forbes*, 2000; *Pancheva et al.*, 2006; *Takahashi et al.*, 2007; *Liu et al.*, 2010; *Chang et al.*, 2011; *Liu et al.*, 2012; *Gu et al.*, 2014]. These waves originate in the lower atmosphere, and with increasing altitude their amplitudes increase while the background densities decrease. Some of the waves are able to penetrate into the *E* region, and thereby, they can modify the dynamo and subsequently cause the variations in the *F* region ionosphere [*Chang et al.*, 2010]. Although some planetary-scale waves are confined to the middle atmosphere, their signatures could be carried into higher altitudes beyond the mesopause through the interactions with atmospheric tides [e.g., *Teitelbaum and Vial*, 1991; *Liu et al.*, 2010; *England et al.*, 2012].

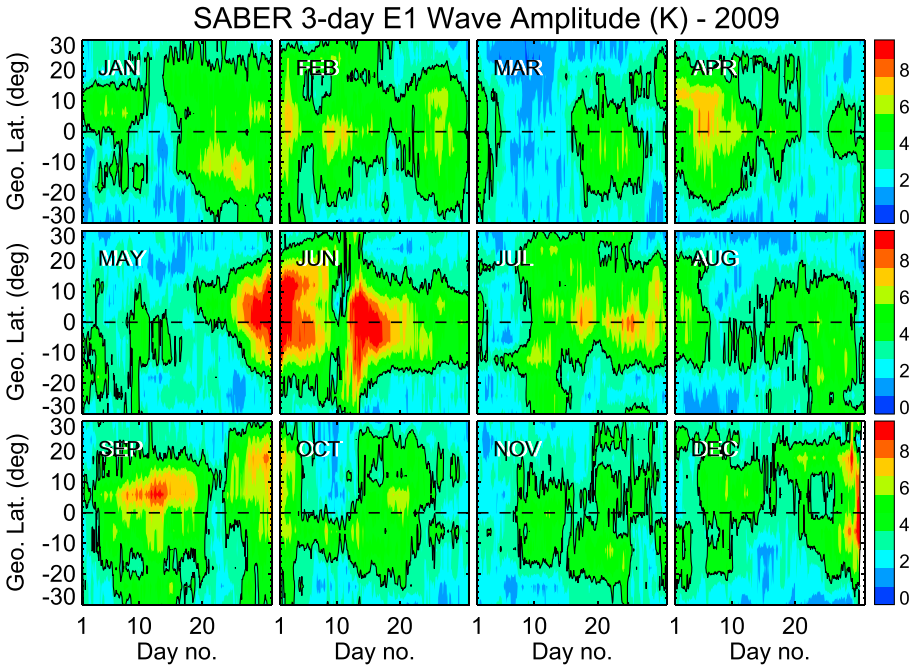

Figure 1. Amplitudes of the 3 day waves for the eastward propagating zonal wave number 1 (*E*1) component as determined from the SABER temperature observations at 98 km altitude during 2009. The contour lines on the plot mark the level of 4 K in temperature.

Kelvin waves are one type of equatorial planetary-scale waves that are generated by the latent heat release in the troposphere [*Holton*, 1973; *Salby and Garcia*, 1987]. They are trapped at low latitudes, having the largest amplitudes at the equator. Away from the equator, the wave amplitudes decrease with increasing latitudes following a Gaussian-like profile [e.g., *Davis et al.*, 2012]. Kelvin waves propagate eastward with respect to the background flow, and they are characterized by wind perturbations mainly in the zonal direction with nonzero meridional wind components observed away from the equator [e.g., *Riggin et al.*, 1997]. Kelvin waves are categorized into three classes. "Slow" Kelvin waves have the longest periods in the range of 15–20 days [*Wallace and Kousky*, 1968] and short vertical wavelengths of ~10 km, meaning they are unable to propagate above the stratosphere. "Fast" Kelvin waves have shorter periods in the range of 6–10 days and larger vertical wavelengths of ~20 km [*Hirota*, 1979]. "Ultrafast" Kelvin waves (UFKWs) have the shortest periods of 2.5–5 days, and their vertical wavelengths have been observed to be ~40 km [*Salby et al.*, 1984]. The amplitudes of UFKWs can reach up to 40 m s^{-1} in the zonal winds and 6 K in the temperatures in the mesosphere and lower thermosphere (MLT) [*Davis et al.*, 2012]. Zonal wave numbers of 1–3 have all been observed, where wave number 1 is most common [e.g., *Lieberman and Riggin*, 1997]. Wave number 1 UFKWs occur intermittently throughout the whole year but have been reported to be observed most often during January–February and June–August [*Vincent*, 1993; *Davis et al.*, 2012; *Gu et al.*, 2014]. The wave number 1 waves have the zonal phase velocity ~150 m s^{-1}, and this combined with the vertical wavelength of ~40 km would allow for the waves to penetrate into the thermosphere [e.g., *Forbes*, 2000; *Takahashi et al.*, 2007; *England et al.*, 2012]. It is thus possible that the UFKWs can directly influence the conditions in the equatorial ionosphere.

The possibility that UFKWs can penetrate into the *F* region altitudes has been supported by some modeling studies [*Chang et al.*, 2010], although other simulation results suggest that the waves should dissipate below these altitudes [e.g., *Pogoreltsev et al.*, 2007]. Observational studies have also reported examples of UFKWs propagating into the thermosphere [e.g., *Takahashi et al.*, 2006; *England et al.*, 2012; *Gu et al.*, 2014]. For example, *Takahashi et al.* [2006] found for one case that the minimum virtual height and the maximum critical frequency of the ionosphere have a 3 day periodic variation that occurs at the same time as the 3 day UFKW in the atmosphere. The study suggested that the observed ionospheric variation was produced through the direct penetration of the UFKW into the thermosphere and subsequent modulation of the ionospheric dynamo. *Gu et al.* [2014] examined the ionospheric response to wave number 1 UFKWs using 1 year

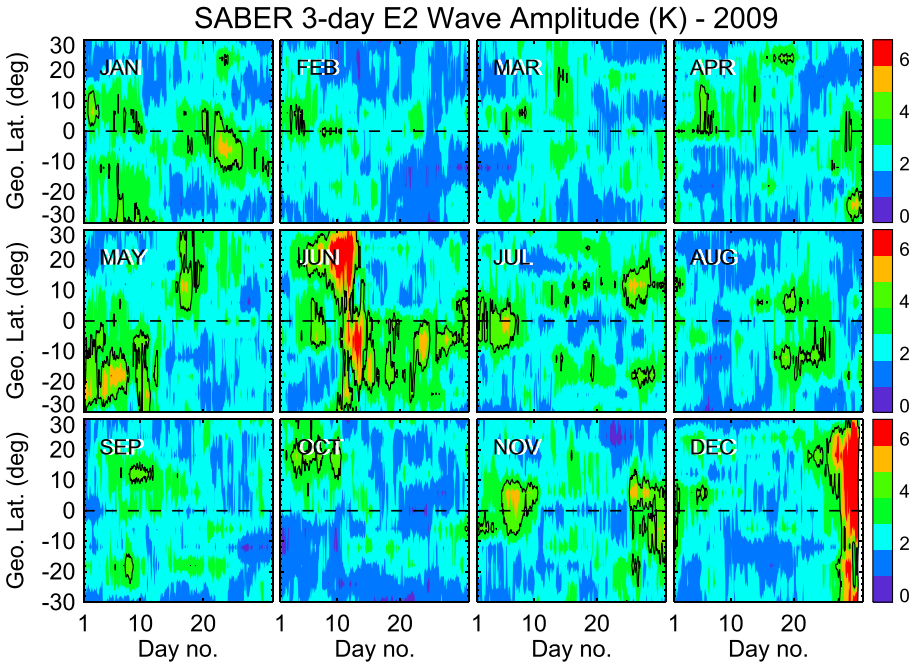

Figure 2. Same as Figure 1 but for the wave number 2 (*E*2).

of data and showed that each large-amplitude wave number 1 UFKW event produced a 3 day wave number 1 response in ionospheric total electron content (TEC). However, it is evident from a simple analysis of UFKWs and ionospheric variations that not all UFKWs produce an ionospheric response. Basic questions such as how often do UFKWs produce global-scale ionospheric signatures and do any properties of these waves or the background atmospheric conditions affect the ability of these waves to impact the ionosphere have never been addressed in a rigorous, statistical way. A comprehensive survey of many UFKW events that uses a long-term observational data set is needed in order to assess the importance of UFKWs on the

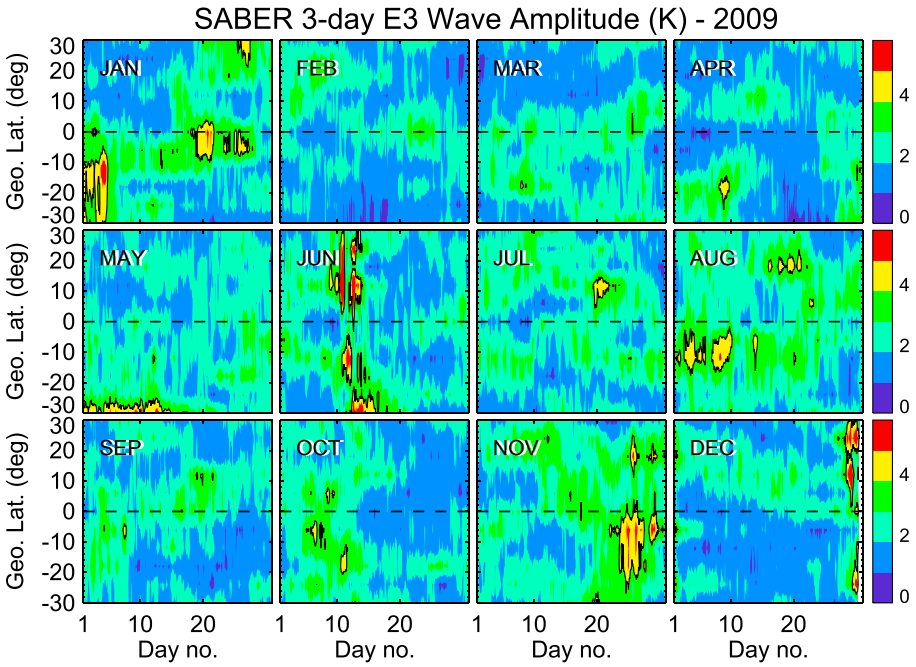

Figure 3. Same as Figures 1 and 2 but for the wave number 3 (*E*3).

Table 1. Total Events of 3 Day Waves Identified From the SABER Temperature Observations at 98 km Altitude for Three Wave numbers Over 2002–2012

Year	Wave Number 1 (*E*1)	Wave Number 2 (*E*2)	Wave Number 3 (*E*3)	Total
2002	17	7	3	27
2003	20	3	3	26
2004	16	3	5	24
2005	15	5	8	28
2006	16	5	4	25
2007	18	10	9	37
2008	16	4	3	23
2009	20	6	5	31
2010	11	4	4	19
2011	16	6	3	25
2012	21	10	4	35
Total	186	63	51	300

ionospheric variations. The survey will need to evaluate for each case whether the waves have the corresponding variations in the equatorial ionosphere.

Here we analyze coincident 3 day variations in observations of both the atmosphere and ionosphere over 11 years from 2002 to 2012. A total of 300 cases of quasi 3 day (hereafter referred to as 3 day) planetary-scale waves with the eastward propagating zonal wave numbers of 1–3 (*E*1–*E*3) are all identified from the global atmospheric temperature observations by the Sounding of the Atmosphere using Broadband Emission Radiometry (SABER) instrument operated on the Thermosphere Ionosphere and Mesosphere Electric Dynamics (TIMED) satellite. The corresponding variations with the same periods and wave numbers in the equatorial ionosphere are searched using the global TEC observations by the International GNSS Service (IGS) (GNSS: Global Navigation Satellite System) ground-based GPS network. These many cases of 3 day waves and ionospheric variations form a large database. By using the database, we determine which 3 day waves affect the ionosphere and what their statistical properties are. This allows us to examine the importance and quantify the frequency of atmospheric UFKW impacts on the day-to-day variations of the equatorial ionosphere from a statistical perspective.

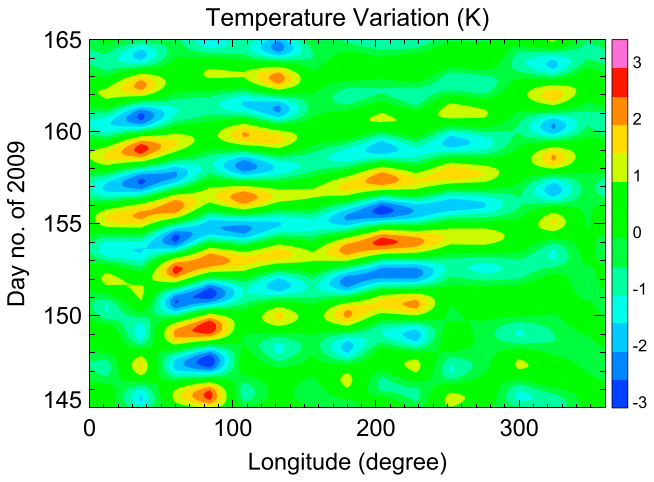

Figure 4. Longitude-time reconstruction of the 3 day wave from the SABER temperatures measured over ±10° latitude at 98 km altitude through days 145–165 of 2009 (25 May to 14 June). Over days 150–160, the eastward propagation of this wave as a function of time is seen. At a single point of time, the wave appears to have a zonal wave number of 1.

2. Data and Analyses

2.1. Atmospheric 3 Day Waves

This study uses v1.07 of the Level 2 kinetic temperature data measured by TIMED/SABER in the altitude range of 70–120 km covering the years of 2002–2012. The measurements by SABER span all longitudes in 1 day, and they are available at two local times separated by ~12 h in the equatorial region. Because the precession rate of the TIMED satellite is relatively slow (~3°/d), the local time differences between adjacent days of observations are negligible. This allows for both the period and zonal wave number of a short-period planetary wave to be determined using only a few days of data. Indeed, the SABER data have been used successfully for studies of short-period

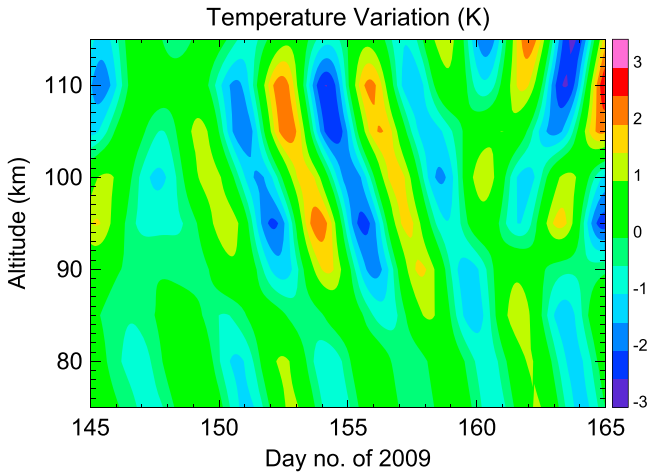

Figure 5. Altitude-time reconstruction of the 3 day wave from the SABER temperature measurements over ±10° latitude throughout days 145–165 of 2009 (25 May to 14 June). The downward phase between days 150 and 160 suggests the upward propagation of this wave. Using the phase propagation, the vertical wavelength of the wave is estimated to be 31–41 km.

planetary-scale waves including the 2, 3, and 5 day waves [e.g., *Forbes et al.*, 2009; *Pancheva et al.*, 2010; *England et al.*, 2012].

For this study, the occurrences of 3 day waves in the low-latitude MLT region are identified from the SABER temperature data. Because the UFKWs are trapped in the equatorial region, only data between ±30° latitude are used. The selected data are grouped into latitude bands 10° wide stepped by 5°. In each band, the data are binned in 24° longitude and 1.6 h UT time intervals (approximately the spatial/temporal resolution of TIMED orbit). The amplitude of a given wave period and zonal wave number is then calculated through the 2-D least squares planetary-scale wave analysis described by *Wu et al.* [1995]. Most 3 day waves are known to have a lifetime of ~10 days [e.g., *Takahashi et al.*, 2009], so the analysis is performed on a 10 day running window stepped by 1.6 h throughout the whole data set. The UFKWs have been observed to have the periods from 2.5 to 4.5 days [e.g., *Forbes*, 2000; *Davis et al.*, 2012], so our analysis is applied to include this range of periods. For one 10 day window, the wave amplitude is determined using the maximum amplitude of a given period between 2.5 and 4.5 days. The eastward zonal wave numbers of 1–3 have all been observed [e.g., *Lieberman and Riggin*, 1997], so they are separately analyzed in this analysis. It should be noted that other planetary-scale waves such as Rossby-gravity waves have the same periods and wave numbers as the UFKWs. They also occur at low latitudes and have the same vertical wavelengths and phase speeds as UFKWs and thus may propagate upward and affect the ionosphere. This analysis therefore includes both pure UFKWs and Rossby-gravity waves that also match the selection criteria described herein.

Figure 1 shows an example of the observed amplitudes of the 3 day waves in temperatures at 98 km altitude for the *E*1 wave number 1 throughout 2009. Twenty events each lasts for about 10 days are seen above an amplitude threshold of 4 K, with several events having amplitudes as high as 10 K. A threshold of 4 K is used here as this is found to be the level at which the properties of the UFKWs (e.g., vertical wavelength) can be reliably determined in our analysis. Because the UFKWs have the maximum amplitudes near the equator, the waves that peak at ≥20° latitude are not considered in this study. The study also excludes the cases when the wave signatures are not persistent (lifetime of the waves at the 4 K threshold are shorter than 5 days).

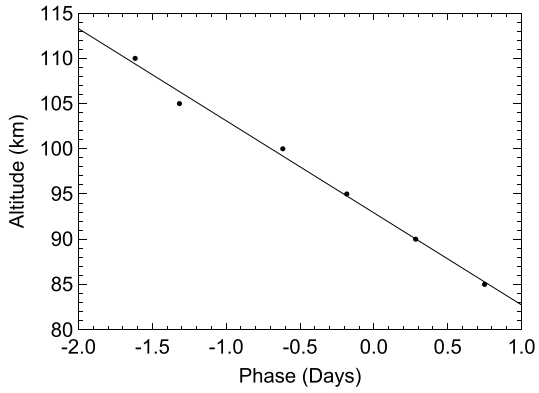

Figure 6. The phase of the 3 day wave as a function of altitude over days 150–160 of 2009 (30 May to 9 June). The straight line is from the best fits.

Similarly, the 3 day waves are identified for the *E*2 and *E*3 wave numbers. Their amplitudes are presented in Figures 2 and 3. Compared to Figure 1, the *E*2 and *E*3 waves have the smaller amplitudes and occur less frequently at a 4 K detection threshold.

We have identified all events of the 3 day waves throughout 2002–2012 (summarized in Table 1). In total, the 3 day waves are identified for 300 cases, with 186 cases for the *E*1 wave number, 63 cases for the *E*2, and 51 cases for the *E*3. The

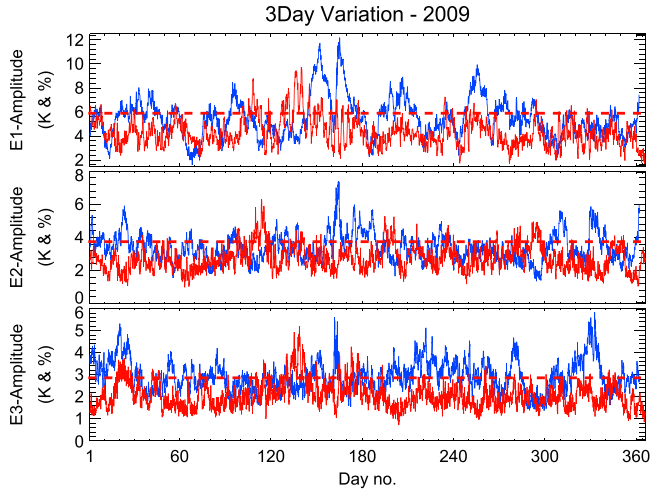

Figure 7. Normalized 3 day variations in TECs (% relative to the mean values), presented in the red color for the zonal wave number 1 (*E*1), zonal wave number 2 (*E*2), and zonal wave number 3 (*E*3) during 2009. The red dashed lines denote the 90th percentiles of these TEC variations. The 3 day wave amplitudes in temperatures are presented in the blue color.

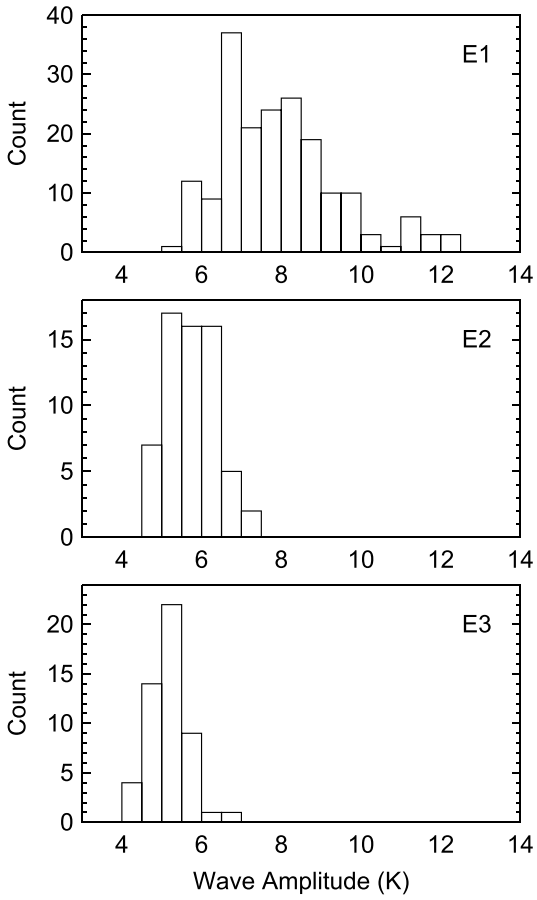

Figure 8. Histograms of the 3 day wave amplitudes in temperatures at 98 km altitude. The histograms are for the eastward wave number 1 (*E*1), wave number 2 (*E*2), and wave number 3 (*E*3).

*E*1 wave is the most often observed, being consistent with the signatures of UFKWs that have been reported [e.g., *Lieberman and Riggin*, 1997]. The *E*2 and *E*3 wave numbers are also observed, as expected based on previous studies [e.g., *Lieberman and Riggin*, 1997].

The SABER data are also used to characterize the properties of the 3 day waves for each of the cases identified. Figure 4 shows an example of the longitudinal propagation of the case during 25 May to 14 June 2009. The variations in temperatures at 98 km altitude are averaged over ±10° latitude, where the wave amplitude peaks, and are presented as a function of longitude. Over the days 150–160 interval, the wave clearly propagates eastward. At a single point in time, the wave appears to have a zonal wave number of 1. These confirm the presence of the *E*1 wave number UFKW signatures as reported before [e.g., *Takahashi et al.*, 2009; *Davis et al.*, 2012].

Figure 5 gives an example of the determination of the vertical wavelength for the same case shown in Figure 4. The wave amplitudes between ±10° latitude are plotted versus altitude and time. The figure shows that the wave amplitude varies as a function of altitude in the range of 75–115 km throughout the time interval of days 150–160. Over these days, the phase is downward, suggesting the upward propagation of the wave. As the wave propagates upward, the phase of the wave changes with altitude. Using this propagation, the vertical wavelength can be estimated. The phase as a function of altitude is plotted (see Figure 6), and also plotted is the best fit straight line. The slope of this line indicates that the vertical wavelength is ~31–41 km (where the uncertainty is determined by the uncertainty in the slope and period of this wave). This propagation and vertical wavelength analysis has been repeated for each of the 300 wave events identified.

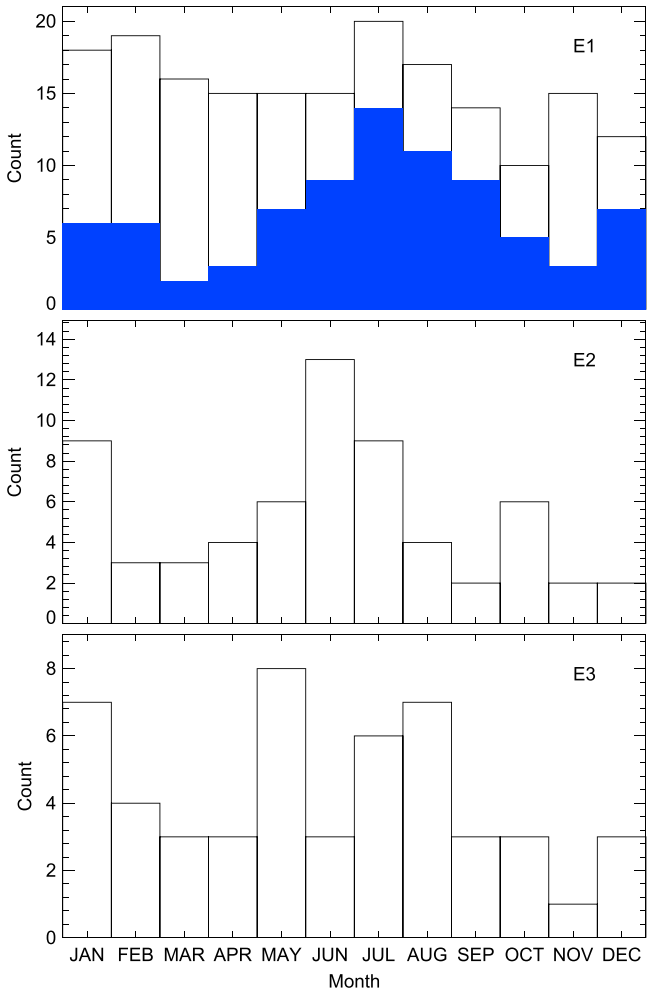

Figure 9. Histograms of the 3 day wave occurrences for the *E*1, *E*2, and *E*3 wave numbers. For the *E*1, the large-amplitude waves (>8 K) are plotted in the blue color.

The Kelvin wave dispersion relation [e.g., *Holton et al.*, 2001] is expressed as

$$\lambda_z = N[\frac{\lambda_x}{\tau} - \bar{u}] \quad (1)$$

where λ_z is the vertical wavelength, N is the Brunt-Väisälä period (~300 s in the MLT region), λ_x is the horizontal wavelength (λ_x = 40,000 km for wave number 1; 20,000 km for wave number 2; and 13,300 km for wave number 3), τ is the wave period, and $\bar{u}$ is the zonal mean zonal wind. From this relation, a vertical wavelength of 45 km for a 3.5 day *E*1 wave number 1 UFKW wave is found if we use the zonal mean zonal wind of −18 m s^{-1} as measured by TIMED/TIMED Doppler Interferometer (TIDI) at 98 km altitude over the 60 day interval in May–June 2009. *Forbes et al.* [2009] used a zonal mean wind of 0 in their calculations, and they found that the vertical wavelength for $\bar{u} = 0$ differs only slightly from those where rough estimates of climatological values are used. This wavelength is close to the range of vertical wavelengths determined from the vertical propagation shown in Figure 5. This is also in general agreement with the vertical wavelengths reported in previous studies [e.g., *Salby et al.*, 1984; *Davis et al.*, 2012].

2.2. Ionospheric 3 Day Variations

The global TEC maps from IGS provide the values of TEC on latitude-longitude grids of 2.5° × 5° at every 2 h of UT time. These maps incorporate the TEC measurements made by the widely distributed network of ground-based GPS receivers. Data gaps, such as those over the oceans where the GPS occultations are not available, are filled in through interpolations and data assimilations [*Mannucci et al.*, 1998]. The IGS global TEC maps have been used in case studies for investigating the ionospheric variations in relation to atmospheric planetary-scale waves [e.g., *Liu et al.*, 2012; *Gu et al.*, 2014]. For this study, the 3 day variations in the equatorial ionosphere and the correspondence of these to each of the 300 3 day waves identified are investigated.

Similar to the SABER data, the IGS global TEC maps generated at JPL are analyzed using the same analysis method as described by *Wu et al.* [1995]. Here we extend the analysis of *Gu et al.* [2014] to include wave numbers 1 through 3 and for all years from 2002 to 2012. For the analysis, at each magnetic latitude (10° wide stepped by 5°) the TEC values at a fixed LT (1600 LT is set for this analysis as the ionosphere is dense, and this LT is away from the rapid changes that occur around sunset) are binned at 2 h UT and 30° longitude intervals. The data are then used to calculate the amplitude of the variation for a given period and wave number using the least squares fits. As with the 3 day waves, the periods between 2.5 and 4.5 days are included and wave numbers of 1–3 are analyzed separately. The analysis is also performed on a 10 day running window throughout the entire data set. In order to remove the changes of the background ionosphere, the variations are finally normalized to the mean values.

Figure 7 presents the calculated amplitudes of 3 day variations in TECs for three wave numbers during 2009. The maximum values between ±20° magnetic latitude are presented. The figure shows that above the

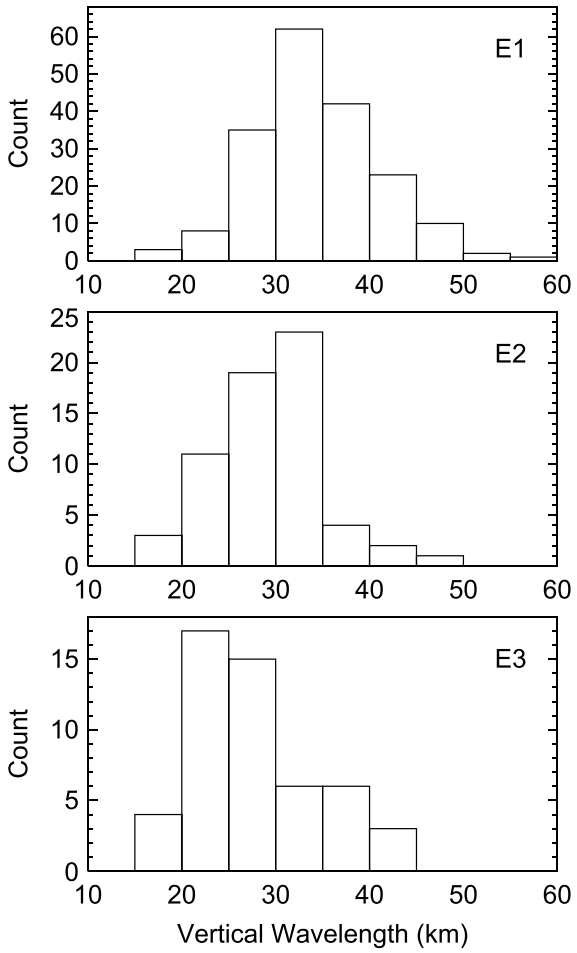

Figure 10. Histograms of the 3 day wave vertical wavelengths for the *E*1, *E*2, and *E*3 wave numbers as calculated using the altitude-time reconstructions of the waves from the SABER temperature measurements.

90th percentile threshold the TEC variations coincide with the atmospheric 3 day waves for some cases. A detailed comparison between the two will be discussed in detail in section 3.

3. Results and Discussions

3.1. Properties of 3 Day Waves

Using the 300 3 day wave events found from 2002 to 2012, we are able to study their amplitudes and vertical wavelengths in a statistical manner.

3.1.1. Amplitudes

Figure 8 shows histograms of the occurrence of different amplitude waves for three wave numbers. For the *E*1 wave number, the modal amplitude is 6.5–7 K, corresponding to 37 cases (20% of the *E*1). The mean amplitude is 7.9 K for the *E*1, with the standard deviation of 1.5 K. For the *E*2 and *E*3, their mean amplitudes and standard deviations are 5.7 K and 0.6 K and 5.1 K and 0.5 K. The figure shows again that the largest-amplitude 3 day waves are almost exclusively *E*1. For all three wave numbers, there is a single central peak in the distribution of amplitudes.

The occurrence rates of 3 day waves have been determined based on a temperature threshold of 4 K at 98 km altitude. This number is equal to the smallest value that could be used and still permit us to identify the vertical propagation of each wave across a sufficient range of altitude to determine the vertical wavelength and to confirm its propagation and wave number using a Hovmöller diagram such as Figure 4, thus allowing us to obtain the largest number of events. Nonetheless, this threshold may have some impact on the histograms shown in Figure 8. For the *E*1 case, this threshold is almost the same as the smallest amplitude of the *E*1, and the amplitudes of the waves form a central peak distribution (see Figure 8) which does not appear to be cut off by this threshold; thus, it appears as though this study includes a truly representative sample of the *E*1 events. The threshold is smaller than the mean amplitudes of the *E*2 and *E*3 wave numbers, but a significant portion of the population is found with amplitudes just above 4 K. It is thus possible that this study only includes *E*2 and *E*3 events of relatively large amplitude (relative to all *E*2 and *E*3 waves).

Figure 9 presents the occurrences of all 3 day waves identified in each month. For the *E*1 events, the wave occurs with almost equal frequency during each month of the year and no clear seasonal dependence is seen. This is in contrast with the seasonal behavior reported by previous studies [e.g., *Vincent*, 1993; *Davis et al.*, 2012; *Gu et al.*, 2014]. If we exclude all waves with amplitudes below the mean (i.e., include only those with amplitudes >8 K), a seasonal dependence is found (shown by the blue bars). For this sample of only the largest-amplitude *E*1 waves, the most frequent occurrences are during June/July/August and December /January/February. Similar seasonal dependences are seen for the *E*2 and *E*3 wave numbers, having the largest wave occurrences in January–February and May–August during solstices. It may be reasonable to suppose that this apparent seasonal behavior may be linked to the selection of only high-amplitude *E*2 and *E*3 described above, although this cannot be determined from these results alone.

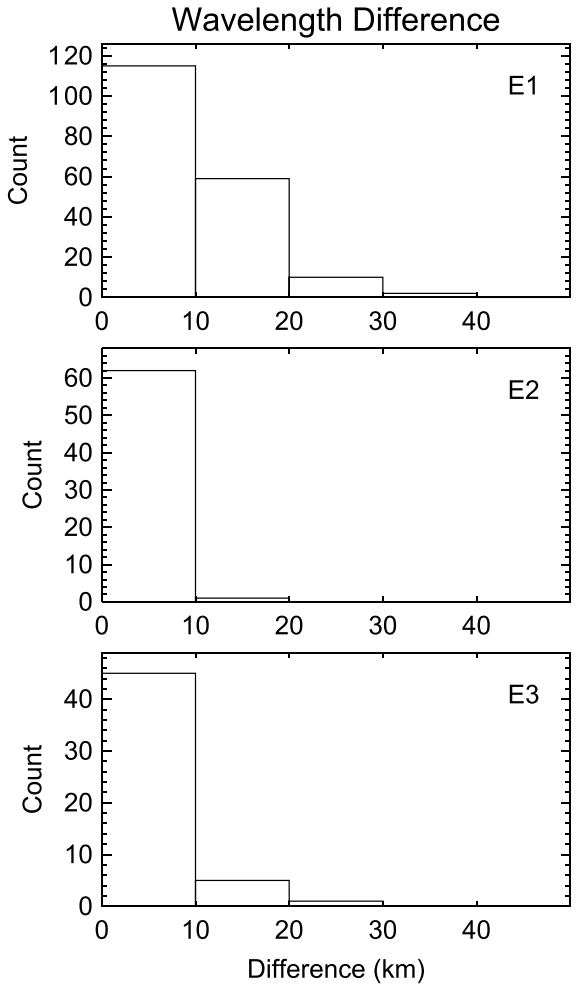

Figure 11. Histograms of the vertical wavelength differences between the calculated values from the SABER temperature observations and the theoretical results using the Kelvin wave dispersion relation.

3.1.2. Vertical Wavelengths

Figure 10 shows the histograms of the calculated vertical wavelengths for all cases (an example of the calculation for one case has been shown in Figures 5 and 6). The mean wavelengths of the *E*1, *E*2, and *E*3 wave numbers are 34 km, 29 km, and 27 km with the standard deviations of 6.5 km, 5.6 km, and 6.7 km, respectively. The *E*1 wave has the longest wavelength, and the *E*3 has the shortest wavelength, as would be suggested by the dispersion relation for UFKWs. The mean value of the *E*1 wavelengths is also within the range of UFKWs that have been reported in previous studies [e.g., *Forbes*, 2000; *Davis et al.*, 2012]. However, the difference in the mean vertical wavelength between *E*1, *E*2, and *E*3 is perhaps smaller than expected from the dispersion relation alone (which suggests that *E*2 and *E*3 should have one half and one third the wavelength of *E*1 for the same period and background wind).

Given this apparent discrepancy, these calculated vertical wavelengths have been compared to the theoretical values that are estimated using the Kelvin wave dispersion relation and zonal mean zonal winds from TIMED/TIDI at 98 km altitude, averaged over a 60 day time interval and the same latitude range as the vertical wavelengths were determined. The differences between them are presented in Figure 11 as the histograms. These show that for most cases, the wavelengths agree with the theoretical results. For the *E*2 and *E*3, almost all are within 10 km of the theoretical values. For the *E*1, a significant number of cases are seen to differ by between 10 and 20 km. These occur at wavelengths both longer and shorter than the theoretical values. The reason for this discrepancy is not clear, but it may be related to simplifications such as using a single zonal mean wind value (98 km altitude used here).

Given that almost all of the *E*2 and *E*3 included in this study have vertical wavelengths consistent with the background wind conditions (follow the wave dispersion), and yet their mean values are larger than expected, it is possible that only the longest vertical wavelength *E*2 and *E*3 waves are detected at the 4 K threshold. This would be consistent with the observation noted above that it is possible only the largest-amplitude *E*2 and *E*3 events are being identified, given that there is a general correlation between wavelength and amplitude because the amplitude is limited by eddy diffusion which goes as the inverse of the square of the vertical wavelength.

3.2. Correspondence of Ionospheric Variations to 3 Day Waves

Together, Figure 7 and 1–3 show that for 2009 many significant (above the 90th percentile) 3 day TEC variations correspond to 3 day waves. In Figure 12 and Table 2, the correspondence is illustrated and summarized for each year from 2002 to 2012. This counts for a total of 199 (66%) events of 3 day waves. The events are for 121 cases of the *E*1 wave number, 42 cases of the *E*2, and 36 cases of the *E*3, accounting for 65%, 67%, and 71% of the total event of waves of one wave number. These similar percentages indicate that all of the wave

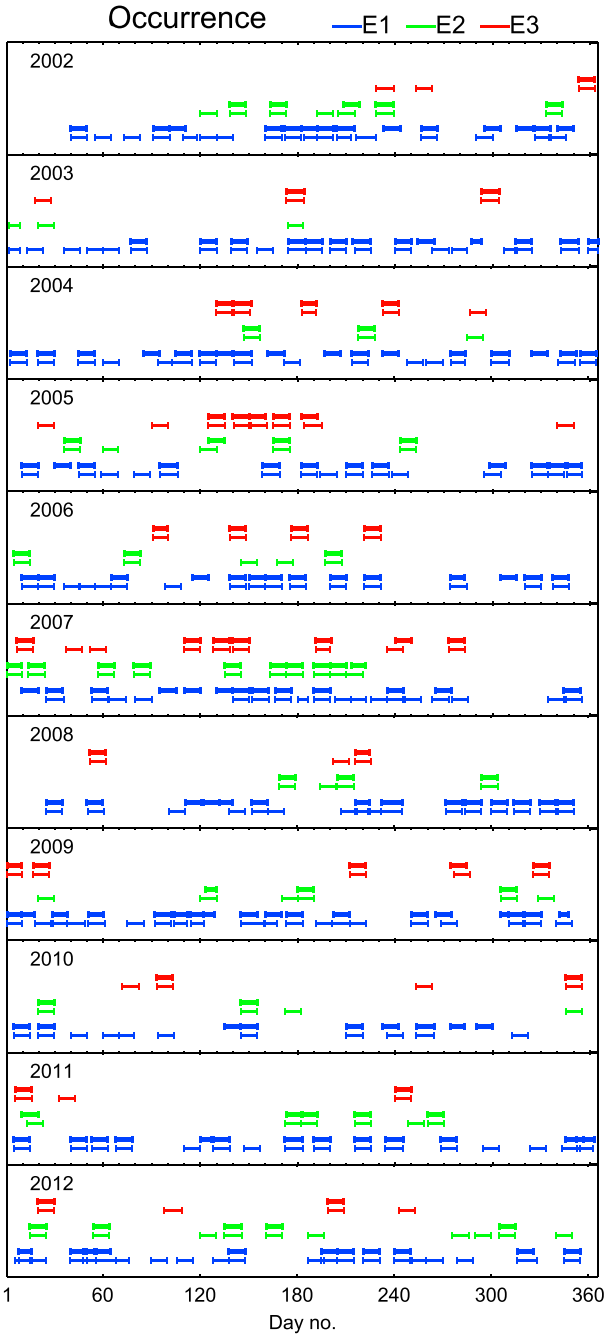

Figure 12. Correspondence between the TEC variations and the 3 day waves for each year through 2002–2012. Horizontal lines mark the TEC variations (thicker lines) and the waves (thin lines below), and different colors are for different wave numbers. Note that for the *E*1 wave number, all TEC variations are included (for some variations there are no 3 day *E*1 waves observed). These are for the total of 28 variations throughout these years.

numbers considered here are of the similar importance in driving ionospheric variations. No single wave number has an ionospheric response more often than the others.

Using the model simulations, *Yue et al.* [2013] have found that both the magnetic field strength and the magnetic dip angle have multiple zonal wave numbers, of which the stationary zonal wave number 1 (S1) is the largest. The interaction of this with the 3 day wave in the atmosphere would produce additional zonal wave numbers in the ionosphere (sums and differences) as

$$E1 \pm S1 = S0, E2$$
$$E2 \pm S1 = E1, E3$$
$$E3 \pm S1 = E2, E4$$

The *E*1 wave should always produce an *E*1 ionospheric variation, but following *Yue et al.* [2013] may also produce a weaker signature at *E*2 TEC. Similarly, the *E*2 (*E*3) wave produces an *E*2 (*E*3) TEC signature but may also produce a weaker signature at *E*1 (*E*2) and *E*3 (*E*4) in TEC. Given that the *E*1 wave has large amplitudes (the *E*2 wave amplitude is, in general, smaller than the *E*1, and the *E*3 wave amplitude is, in general, smaller than the *E*2), the *E*2 wave should not produce many *E*1 TEC variations that are significant. It is thus possible that most of the *E*1 TEC variations are caused by the *E*1 waves, which will be investigated further below. However, given their relative amplitudes, the *E*1 wave may produce significant *E*2 TEC variations, and the *E*2 wave may produce significant *E*3 TEC variations. For the *E*2 and *E*3 wave numbers, we can identify the TEC variations that correspond to the same wave number waves but often cannot attribute these variations to the parent waves, as *E*1 may also be present in the atmosphere. Also, given that in this study, where a 4 K threshold has been used to identify waves in the SABER data, we cannot identify all wave events for the two wave numbers, we cannot determine whether the *E*2 and *E*3 TEC variations are caused by the waves of the corresponding wave numbers. However, given that *E*2 and *E*3 waves produce *E*2 and *E*3 TEC variations, it is of interest to examine the correspondence of *E*1, *E*2, and *E*3 TEC variations with known *E*1, *E*2, and *E*3 wave events.

Table 2. Total Numbers of 3 Day Waves That Have Corresponding Variations in TECs (Above 90th Percentiles) Throughout 2002–2012

Year	Wave Number 1 (*E*1)	Wave Number 2 (*E*2)	Wave Number 3 (*E*3)	Total
2002	11	5	1	17
2003	11	0	2	13
2004	11	2	4	17
2005	11	4	5	20
2006	12	3	4	19
2007	9	10	7	26
2008	11	3	2	16
2009	15	3	5	23
2010	6	2	2	10
2011	12	5	2	19
2012	12	5	2	19
Total	121 (65%)	42 (67%)	36 (71%)	199 (66%)

The 3 day waves that have the corresponding TEC variations are now further analyzed. The waves are categorized according to different properties, and the numbers of waves in each category are counted. As no strong trend with wave number is seen and to improve the statistics, we have combined the events for the three wave numbers. As listed in Table 3, the percentages of these waves (relative to the total numbers of waves) are similar between each group. Specifically, the waves of different wavelength ranges have almost the same percentages (~66%) of corresponding TEC variations. The percentage is slightly larger for the large-amplitude waves (>8 K) than the small-amplitude waves (<6 K) at the values of 77% and 62%. It is also slightly larger at solstices (71%) than at equinoxes (58%). The percentage is equal to 67% during 2002 and 2003 at solar minimum, being larger than the value of 57% in 2008–2010 at solar maximum. These indicate that the waves that can affect the ionosphere are not determined by vertical wavelength. However, it appears to be more common for a large-amplitude 3 day wave to create such a large-amplitude variation in the ionosphere, and this occurs more often at solstices and solar minimum.

The corresponding TEC variations are determined statistically significant above the 90th percentile levels. The levels are different for the three wave numbers (specifically, it is highest at 6% of change for *E*1, at 3.6% for *E*2, and lowest at 2.8% for *E*3). As may be expected, for the changing threshold the number of correspondences between the TEC variations and the 3 day waves varies. To examine the impact of this, we repeat the analysis shown in Figure 12 and Table 2 for ionospheric perturbations equal to ~4.2% of change, which is the mean value that corresponds to the 90th percentile of three wave numbers. The results

Table 3. Total Numbers of 3 Day Waves and the Numbers (Percentages) of Corresponding TEC Variations Through 2002–2012 for Various Categorizes of the Waves[a]

Category	Waves	TEC Variations
Long vertical wavelength (>35 km)	81	54 (67%)
Normal vertical wavelength (25–35 km)	173	115 (66%)
Short vertical wavelength (<25 km)	46	30 (65%)
Large wave amplitude (>8 K)	75	58 (77%)
Normal wave amplitude (6–8 K)	123	78 (63%)
Small wave amplitude (<6 K)	102	63 (62%)
Equinoxes	124	72 (58%)
Solstices	183	130 (71%)
Solar maximum	53	30 (57%)
Solar minimum	73	49 (67%)

[a]The TEC variations are above 90th percentiles.

Table 4. Total Numbers of 3 Day Waves and the Numbers (Percentages) of Corresponding TEC Variations Through 2002–2012 for Various Categorizes of the Waves[a]

Category	Waves	TEC Variations
Long vertical wavelength (>35 km)	81	63 (78%)
Normal vertical wavelength (25–35 km)	173	121 (70%)
Short vertical wavelength (<25 km)	46	13 (28%)
Large wave amplitude (>8 K)	75	68 (91%)
Normal wave amplitude (6–8 K)	123	96 (78%)
Small wave amplitude (<6 K)	102	33 (32%)
Equinoxes	124	79 (64%)
Solstices	183	121 (66%)
Solar maximum	53	33 (62%)
Solar minimum	73	47 (64%)

[a]The TEC variations are for the level of 4.2% change.

are shown in Table 4. Seventy-eight percent of the long vertical wavelength waves (>35 km) have corresponding TEC variations, while only 28% of the short wavelength waves (<25 km) have the correspondence. For the large-amplitude waves (>8 K), 91% of them coincide with the TEC variations, but only 32% of the small-amplitude waves (<6 K) have the corresponding TEC variations. The frequency at which the waves impact the ionosphere at this TEC perturbation threshold is thus ~3 times larger for the large-amplitude and long vertical wavelength waves than the small-amplitude and short vertical wavelength waves. However, the frequency is almost the same between equinoxes and solstices (64% and 66%), and it is also the same at solar maximum and solar minimum (62% and 64%), suggesting no seasonal and solar cycle dependence of the occurrence of waves that propagate and impact the ionosphere. These show a clear trend, with the waves that impact the ionosphere are most often of large amplitudes and long vertical wavelengths. This indicates that the long wavelength and large-amplitude 3 day waves are most important in driving ionospheric variations above a threshold amplitude (rather than above a threshold statistical significance).

To investigate the potential causal relationship between *E*1 wave events and TEC variations further, we have also identified the *E*1 TEC variations that do not correspond to any *E*1 waves (all *E*1 TEC variations are illustrated in Figure 12). These count for only 28 cases, at 19% of the total *E*1 TEC variations. All of the other 81% of *E*1 TEC variations observed over this 11 year time interval are coincident with *E*1 atmospheric waves. It is possible that some portion of these 28 cases are caused by *E*2 waves or variations in solar and magnetospheric forcing, but an exhaustive search for the origin of each of these 28 events is beyond the scope of this study.

4. Conclusions

This paper presents a comprehensive survey of atmospheric quasi 3 day planetary-scale waves in the MLT region and quantifies the impacts of these waves on the day-to-day variations of the equatorial ionosphere using a statistical analysis. A large database is built, including 300 events of 3 day waves for the eastward propagating zonal wave numbers of 1–3 (*E*1–*E*3) throughout 2002–2012. Among these, 199 cases (66%) of 3 day waves are found to occur coincidently with the variations of the same periods and wave numbers in the equatorial ionosphere.

Occurrence and properties of 3 day waves are determined from the global temperature observations by SABER in the altitude range of 70–100 km. The waves are identified for the total of 300 events with 186 events for the *E*1 wave number, 63 events for the *E*2, and 51 events for the *E*1. Their mean amplitudes and vertical wavelengths are calculated to be 7.9 K and 34 km, 5.7 K and 29 km, and 5.1 K and 27 km, with the standard deviations of 1.5 K and 6.5 km, 0.6 K and 5.6 km, and 0.5 K and 6.7 km for the three wave numbers. The *E*1 wave number is the most often observed, and it has the largest-amplitude and longest vertical wavelength. Although the *E*1 waves do not show a seasonal behavior when all events are included, the large-amplitude cases (>8 K) occur more often during solstices than at equinoxes. The *E*2 and *E*3 wave numbers are also observed to occur most often in January–February and May–August.

The coincident observations of the global TEC distributions are used to identify the corresponding ionospheric variations to the 3 day waves. The variations are found for 121, 42, and 36 cases of the *E*1, *E*2, and *E*3 wave numbers, accounting for 65%, 67%, and 71% of total wave events, respectively. These variations are all statistically significant at 90th percentiles, which on average is equivalent to the change of 4.2% in TEC (relative to the mean TEC). For this level of change, 78% of the long vertical wavelength waves (>35 km) and 91% of the large-amplitude waves (>8 K) are found to have the corresponding TEC variations, while only 28% of the short vertical wavelength waves (<25 km) and 32% of the small-amplitude waves (<6 K) have the corresponding variations. The frequency at which the waves impact the ionosphere is ~3 times larger for the large-amplitude and long vertical wavelength waves than the small-amplitude and short vertical wavelength waves.

The study shows that the long wavelength and large-amplitude 3 day waves are most important in driving the corresponding ionospheric variations above a threshold amplitude. However, the frequencies of the 3 day waves that have corresponding ionospheric variations are almost the same between equinoxes and solstices (64% and 66%) and are also the same between solar maximum and solar minimum (62% and 64%), indicating no seasonal and solar cycle dependence on the frequency at which 3 day waves create impacts on the ionosphere at the threshold TEC perturbation level. This suggests that there is no clear seasonal and solar cycle dependence on the propagation of such waves from the mesopause region to higher altitudes.

Looking closely at the correspondence between *E*1 wave events and *E*1 TEC variations, we see that over the 11 years studied 65% of the time when an *E*1 wave is seen in the atmosphere, an *E*1 TEC variation is seen in the ionosphere. To gain more insights into a possible causal link between these atmospheric waves and ionospheric variations, we investigated all recorded *E*1 TEC variations and found that 81% of all TEC variations occur at the same time as a clear *E*1 wave event in the atmosphere (19% of TEC variation do not correspond to any *E*1 waves). These findings are consistent with the hypothesis that *E*1 wave events are the primary cause of *E*1 TEC variations but that not all *E*1 wave events generate significant *E*1 TEC variations. This may be due to unfavorable atmospheric or ionospheric conditions or some other factors not identified here. As discussed in section 3.2, it is not possible to identify the primary cause of *E*2 and *E*3 TEC variations. However, for the largest *E*2 and *E*3 wave events (those identified in this study), it is interesting that corresponding *E*2 and *E*3 ionospheric variations occur 67% and 71% of the time (similar to the *E*1 variations at 65%). This would also be consistent with the hypothesis that conditions that are favorable for 3 day waves to create ionospheric variations are present approximately two thirds of the time.

Acknowledgments

This research work was supported by the National Aeronautics and Space Administration (NASA) Heliophysics Research program through Award NNX12AD48G. Portions of this research were carried out at the Jet Propulsion Laboratory, California Institute of Technology, under a contract with NASA. The SABER data were obtained from GATS Incorporated at http://saber.gats-inc.com, and the TEC maps were obtained from NASA's Space Physics Data Facility at http://cdaweb.gsfc.nasa.gov. The TIDI data were obtained from http://tidi.engin.umich.edu.

Alan Rodger thanks the reviewers for their assistance in evaluating this paper.

References

Chang, L. C., S. E. Palo, H.-L. Liu, T.-W. Fang, and C. S. Lin (2010), Response of the thermosphere and ionosphere to an ultra fast Kelvin wave, *J. Geophys. Res.*, *115*, A00G04, doi:10.1029/2010JA015453.

Chang, L. C., J.-Y. Liu, and S. E. Palo (2011), Propagating planetary wave coupling in SABER MLT temperatures and GPS TEC during the 2005/2006 austral summer, *J. Geophys. Res.*, *116*, A10324, doi:10.1029/2011JA016687.

Davis, R. N., Y.-W. Chen, S. Miyahara, and N. J. Mitchell (2012), The climatology, propagation and excitation of ultra-fast Kelvin waves as observed by meteor radar, Aura MLS, TRMM and in the Kyushu-GCM, *Atmos. Chem. Phys.*, *12*, 1865–1879, doi:10.5194/acp-12-1865-2012.

England, S. L., G. Liu, Q. Zhou, T. J. Immel, K. K. Kumar, and G. Ramkumar (2012), On the signature of the quasi-three-day wave in the thermosphere during the January 2010 URSI World Day Campaign, *J. Geophys. Res.*, *117*, A06304, doi:10.1029/2012JA017558.

Forbes, J. M. (2000), Wave coupling between the lower and upper atmosphere: Case study of an ultra-fast Kelvin Wave, *J. Atmos. Sol. Terr. Phys.*, *62*, 1603–1621, doi:10.1016/S1364-6826(00)00115-2.

Forbes, J. M., X. Zhang, S. E. Palo, J. Russell, C. J. Mertens, and M. Mlynczak (2009), Kelvin waves in stratosphere, mesosphere and lower thermosphere temperatures as observed by TIMED/SABER during 2002–2006, *Earth Planets Space*, *61*, 447–453.

Gu, S.-Y., X. Dou, J. Lei, T. Li, X. Luan, W. Wan, and J. M. Russell (2014), Ionospheric response to the ultrafast Kelvin wave in the MLT region, *J. Geophys. Res. Space Physics*, *119*, 1369–1380, doi:10.1002/2013JA019086.

Hirota, I. (1979), Kelvin waves in the equatorial middle atmosphere observed by the Nimbus 5. SCR., *J. Atmos. Sci.*, *36*, 217–222, doi:10.1175/1520-0469(1979)036<0217:KWITEM>2.0.CO;2.

Holton, J. R. (1973), On the frequency distribution of atmospheric Kelvin waves, *J. Atmos. Sci.*, *30*, 499–500, doi:10.1175/1520-0469(1973)030<0499:OTFDOA>2.0.CO;2.

Holton, J. R., M. J. Alexander, and M. T. Boehm (2001), Evidence for short vertical wavelength Kelvin waves in the Department of Energy-Atmospheric Radiation Measurement Nauru99 radiosonde data, *J. Geophys. Res.*, *106*, 20,125–20,130, doi:10.1029/2001JD900108.

Laštovička, J. (2006), Forcing of the ionosphere by waves from below, *J. Atmos. Sol. Terr. Phys.*, *68*, 479–497, doi:10.1016/j.jastp.2005.01.018.

Lieberman, R. S., and D. Riggin (1997), High resolution Doppler imager observations of Kelvin waves in the equatorial mesosphere and lower thermosphere, *J. Geophys. Res.*, *102*, 26,117–26,130, doi:10.1029/96JD02902.

Liu, G., T. J. Immel, S. L. England, K. K. Kumar, and G. Ramkumar (2010), Temporal modulation of the four-peaked longitudinal structure of the equatorial ionosphere by the 2 day planetary wave, *J. Geophys. Res.*, *115*, A12338, doi:10.1029/2010JA016071.

Liu, G., S. L. England, T. J. Immel, K. K. Kumar, G. Ramkumar, and L. P. Goncharenko (2012), Signatures of the 3-day wave in the low- and mid-latitude ionosphere during the January 2010 URSI World Day campaign, *J. Geophys. Res.*, *117*, A06305, doi:10.1029/2012JA017588.

Mannucci, A. J., B. D. Wilson, D. N. Yuan, C. H. Ho, U. J. Lindqwister, and T. F. Runge (1998), A global mapping technique for GPS-derived ionospheric total electron content measurements, *Radio Sci.*, *33*, 565–582, doi:10.1029/97RS02707.

Pancheva, D., P. Mukhtarov, B. Andonov, and J. M. Forbes (2010), Global distribution and climatological features of the 5–6-day planetary waves seen in the SABER/TIMED temperatures (2002–2007), *J. Atmos. Sol. Terr. Phys.*, *72*, 26–37, doi:10.1016/j.jastp.2009.10.005.

Pancheva, D. V., et al. (2006), Two-day wave coupling of the low-latitude atmosphere-ionosphere system, *J. Geophys. Res.*, *111*, A07313, doi:10.1029/2005JA011562.

Pogoreltsev, A. I., A. A. Vlasov, K. Fröhlich, and C. Jacobi (2007), Planetary waves in coupling the lower and upper atmosphere, *J. Atmos. Sol. Terr. Phys.*, *69*, 2083–2101, doi:10.1016/j.jastp.2007.05.014.

Riggin, D. M., D. C. Fritts, T. Tsuda, T. Nakamura, and R. A. Vincent (1997), Radar observations of a 3-day Kelvin wave in the equatorial mesosphere, *J. Geophys. Res.*, *102*, 26,141–26,158, doi:10.1029/96JD04011.

Salby, M. L., and R. R. Garcia (1987), Transient response to localized episodic heating in the tropics. Part I: Excitation and short-time near-field behavior, *J. Atmos. Sci.*, *44*, 458–498, doi:10.1175/1520-0469(1987)044<0458:TRTLEH>2.0.CO;2.

Salby, M. L., D. L. Hartmann, P. L. Bailey, and J. C. Gille (1984), Evidence for equatorial Kelvin modes in Nimbus-7 LIMS, *J. Atmos. Sci.*, *41*, 220–235, doi:10.1175/1520-0469(1984)041<0220:EFEKMI>2.0.CO;2.

Takahashi, H., C. M. Wrasse, D. Pancheva, M. A. Abdu, I. S. Batista, L. M. Lima, P. P. Batista, B. R. Clemesha, and K. Shiokawa (2006), Signatures of 3–6 day planetary waves in the equatorial mesosphere and ionosphere, *Ann. Geophys.*, *24*, 3343–3350, doi:10.5194/angeo-24-3343-2006.

Takahashi, H., et al. (2007), Signatures of ultra fast Kelvin waves in the equatorial middle atmosphere and ionosphere, *Geophys. Res. Lett.*, *34*, L11108, doi:10.1029/2007GL029612.

Takahashi, H., et al. (2009), Possible influence of ultra-fast Kelvin wave on the equatorial ionosphere evening uplifting, *Earth Planets Space*, *61*, 455–462.

Teitelbaum, H., and F. Vial (1991), On tidal variability induced by nonlinear interaction with planetary waves, *J. Geophys. Res.*, *96*, 14,169–14,178, doi:10.1029/91JA01019.

Vincent, R. (1993), Long-period motions in the equatorial mesosphere, *J. Atmos. Terr. Phys.*, *55*(7), 1067–1080, doi:10.1016/0021-9169(93)90098-J.

Wallace, J. M., and V. E. Kousky (1968), Observational evidence of Kelvin waves in the tropical stratosphere, *J. Atmos. Sci.*, *25*, 900–907, doi:10.1175/1520-0469(1968)025<0900:OEOKWI>2.0.CO;2.

Wu, D. L., P. B. Hays, and W. R. Skinner (1995), A least squares method for spectral analysis of space-time series, *J. Atmos. Sci.*, *52*, 3501–3511, doi:10.1175/1520-0469(1995)052<3501:ALSMFS>2.0.CO;2.

Yue, J., W. Wang, A. D. Richmond, H.-L. Liu, and L. C. Chang (2013), Wavenumber broadening of the quasi 2 day planetary wave in the ionosphere, *J. Geophys. Res. Space Physics*, *118*, 3515–3526, doi:10.1002/jgra.50307.